Available online at www.sciencedirect.com
SCIENCE DIRECT®
Developmental Biology 270 (2004) 135–145
DEVELOPMENTAL BIOLOGY
www.elsevier.com/locate/ydbio

A stepwise model system for limb regeneration

Tetsuya Endo, Susan V. Bryant, and David M. Gardiner*

Department of Developmental and Cell Biology and the Developmental Biology Center, University of California-Irvine, Irvine, CA 92697, USA

Received for publication 17 December 2003, revised 23 February 2004, accepted 23 February 2004

Available online 15 April 2004

Abstract

The amphibian limb is a model that has provided numerous insights into the principles and mechanisms of tissue and organ regeneration. While later stages of limb regeneration share mechanisms of growth control and patterning with limb development, the formation of a regeneration blastema is controlled by early events that are unique to regeneration. In this study, we present a stepwise experimental system based on induction of limb regeneration from skin wounds that will allow the identification and functional analysis of the molecules controlling this early, critical stage of regeneration. If a nerve is deviated to a skin wound on the side of a limb, an ectopic blastema is induced. If a piece of skin is grafted from the contralateral side of the limb to the wound site concomitantly with nerve deviation, the ectopic blastema continues to grow and forms an ectopic limb. Our analysis of dermal cell migration, contribution, and proliferation indicates that ectopic blastemas are equivalent to blastemas that form in response to limb amputation. Signals from nerves are required to induce formation of both ectopic and normal blastemas, and the diversity of positional information provided by blastema cells derived from opposite sides of the limb induces outgrowth and pattern formation. Hence, this novel and convenient stepwise model allows for the discovery of necessary and sufficient signals and conditions that control blastema formation, growth, and pattern formation during limb regeneration.

Keywords: Regeneration; Ectopic limb; Skin; Wound healing; Dedifferentiation; Cell proliferation; Cell migration; Nerve; Fibroblast; Amphibian

Introduction

Urodele amphibians are unique among adult vertebrates in their ability to regenerate many of their body parts. Among the tissues and organs that can regenerate, the limb has been most extensively studied, providing the basis for current views about the mechanisms regulating tissue and organ regeneration. Successful limb regeneration progresses through a characteristic series of steps, beginning with wound healing, followed by formation of a regeneration blastema, and leading to a redevelopment phase that is a recapitulation of the events that occur during embryonic development (Bryant et al., 2002; Gardiner et al., 1999, 2002). Although the later phase of limb regeneration is equivalent to limb development, the early phase, resulting in the genesis of the blastema, is unique to regeneration. It is this phase that we seek to understand so as to be able to enhance regenerative processes in humans. To gain insight into this phase, we have utilized the ability of salamanders to form ectopic limbs from wounds on the sides, rather than the ends of limbs. Ectopic limb formation will allow the development of a positive assay to identify the steps that lead from wound healing to blastema formation and to eventual limb regeneration.

Ectopic limb formation was documented in experiments by Bodemer (1958, 1959) in the mid-20th century, and expanded upon in recent years (Egar, 1988; Lheureux, 1977; Maden and Holder, 1984; Reynolds et al., 1983). Without intervention, a wound on the side of the limb heals and the skin is regenerated. Bodemer reported that if a nerve was deviated to the site of the wound, outgrowth of an entire extra limb (ectopic limb) could be induced at a reasonably high frequency if wounding was accompanied by extensive trauma. Later studies demonstrated that extensive trauma was not required if a piece of skin (connective tissue fibroblasts) was grafted from the contralateral side of the limb to the wound site in conjunction with a deviated nerve (Lheureux, 1977; Maden and Holder, 1984; Reynolds et al., 1983), although the frequency of full regeneration was variable.

In this paper, we have expanded on these observations and have developed a reproducible stepwise experimental

* Corresponding author. Fax: +1-949-824-5385.
E-mail address: dmgardin@uci.edu (D.M. Gardiner).

0012-1606/$ - see front matter © 2004 Elsevier Inc. All rights reserved.
doi:10.1016/j.ydbio.2004.02.016

system to study regeneration in an ectopic location on a lateral surface of the limb. The important advantage of ectopic regeneration over normal regeneration from an amputation site is that it provides a positive way to assay for the steps necessary to initiate regeneration and to make progress from one step to another. Because normal regeneration always follows amputation unless the process is inhibited, it cannot easily be used to demonstrate the important steps in the process. Having to rely almost exclusively on inhibitory assays is one of the factors that have slowed progress in understanding regeneration. Here we demonstrate that in the first phase of regeneration, nerves play an essential role in dedifferentiation, mobilization, and migration of dermal fibroblasts to form an ectopic blastema. Ectopic blastemas (bumps) formed by nerve deviation alone eventually regress, but are capable of fully regenerating a limb, provided they receive additional signals generated when fibroblasts from the opposite side of the limb are introduced. Hence, bumps provide a simplified and sufficient system for regeneration, and are especially suited for the study of the early unique steps of the process.

Materials and methods

Animals

Axolotls (*Ambystoma mexicanum*) were spawned at either the Indiana University Axolotl Colony or at the University of California, Irvine. Larvae (4.5–8 cm, snout to tail tip) were maintained at 20–22 °C in 20% Holtfreter's solution. Animals were anesthetized in 0.1% MS222 solution for surgical procedures.

Surgical procedures

To induce ectopic blastemas (bumps), a square of skin (1.0–1.5 mm on a side) was removed from the anterior or posterior side of the mid-upper arm, making sure that the underlying muscle was not damaged. A ventral incision was made from the shoulder to the elbow, and the brachial nerve was dissected free and severed at the elbow level. The nerve was rerouted beneath the skin to bring the cut end to the center of the skin wound.

To induce ectopic limbs, skin wounds were made as described above, except that a rectangular piece of skin (1–1.5 × 2–3 mm) was removed. A square piece of skin was removed from the opposite position on the contralateral limb (i.e., posterior for an anterior wound and vice verse) and grafted to the site of the skin wound. Skin grafts were labeled with carbon particles (ink) to confirm that grafted tissues had healed into the host site.

To test if the growth of the bump is nerve-dependent or independent, we performed denervation of bumps. Bumps were made as described above, and at days 6 and 10 after nerve deviation, the 3rd, 4th, and 5th spinal nerves were exposed at the scapula level and severed.

Immunohistochemistry and histology

Limbs were amputated at the shoulder level, fixed overnight in 10% neutral buffered formalin, processed and embedded in paraplast, and sectioned at 10 μm. For BrdU and acetylated-tubulin immunohistochemistry, sections were de-paraffinized and rehydrated in PBS with 0.1% Tween 20 (PBST). BrdU samples were treated with 2 M HCl at 37 °C for 60 min. Sections were incubated with anti-BrdU antibody (Roche, diluted 6:100) or anti-acetylated tubulin antibody (Sigma, diluted 1:1000) for 60 min at room temperature (RT). Sections were washed several times in PBST and incubated with 1:50 alkaline phosphatase (AP)-conjugated anti-mouse IgG (Sigma) at RT for 60 min. Sections were washed with PBST and incubated in NBT/BCIP (Roche) reaction mix for 30 min. For routine histology, sections were stained with either hematoxylin and eosin or Mallory's triple stain (Humason, 1979).

BrdU analysis

We injected BrdU (100 μg/g bodyweight) intraperitoneally on day 13 for growing bumps and on day 21 or 23 for regressing bumps. Bumps were fixed 2 h after BrdU injection. Because the size of the bumps was variable, for growing bumps we selected those that measured 500–600 μm from base to apex (proximal to distal), and for regressing bumps those that measured 600–700 μm. BrdU-labeled mesenchymal cells were counted in each 100-μm band along the proximal to distal axis in unstained longitudinal sections that included the most distal tip of the bump. The total number of cells in each band was counted in the adjacent hematoxylin and eosin-stained section.

DiI labeling

CellTracker CM-DiI (chloromethylbenzamide; Molecular Probes) in ethanol (0.5%) was diluted 1:9 with 0.3 M sucrose containing 0.1% Nile blue sulfate (Li and Muneoka, 1999) and used to label dermal cells adjacent to wounds. To label cells in vivo, small volumes of DiI were injected with a fine glass capillary needle inserted through the intact skin into the space between the skin and the underlying muscle and connective tissues. One day after injection, a skin wound was made adjacent to the location of the DiI-labeled cells (visualized using a fluorescence dissecting microscope). To label cells in vitro, a piece of skin adjacent to a wound was placed dermal surface up in a sterile culture dish. DiI was microinjected into the dermal connective tissue layer multiple times, and the skin was then grafted back to its original location adjacent to the lateral wound. Labeled cells in bumps were observed in sections. In

Table 1
Frequency of bump formation

	N	No bump	Bump
Wound	3	3 (100%)	0 (0%)
Wound + Nerve	40	1 (2%)	39 (98%)
Wound + Nerve + Sham skin graft	4	1 (25%)	3 (75%)
Wound + Sham nerve + Skin graft	3	3 (100%)	0 (0%)

Table 2
Frequency of limb formation

	N	Bump	Limb
Wound + Nerve	19	18 (95%)	1 (5%)
Wound + Nerve + Skin graft	15	4 (27%)	11 (73%)

wounds, DiI-labeled cells were observed and photographed in anesthetized animals using a fluorescence dissecting microscope.

Results

Wound healing, ectopic blastemas (bumps), and ectopic limbs

Lateral wounds are covered rapidly by the epidermis. Trypan blue exclusion data indicate that two out of four wounds are healed within 2 h, and all are healed within 4 h. This time course for epidermal healing is comparable to that of amputated limbs (Carlson et al., 1998). Following epidermal healing, in wounds that did not receive a deviated nerve, the skin regenerates without imperfections and without forming an outgrowth (Table 1).

In contrast to a simple skin wound, when a nerve is deviated to a skin wound on either the anterior or posterior side of the limb (Fig. 1A), a blastema-like outgrowth (bump) is induced (Fig. 1B) at very high frequency in response to signals from the deviated nerve (Table 1; 98%, $n = 40$). Nineteen bumps were observed long enough to determine the fate of the induced bumps, and only one bump continued development into a limb-like structure (Table 2). This bump was induced from a posterior wound and developed a tapering outgrowth with only one digit. All of the other bumps eventually stopped developing, began to regress (Fig. 1C), and eventually could no longer be detected.

When a piece of skin is grafted contralaterally to the site of a skin wound to which a nerve has been deviated (Fig. 1D), the majority of the bumps do not regress, but rather continue to grow (Fig. 1E), and eventually form an ectopic limb (Fig. 1F). Of the 15 bumps formed at wounds with nerves and skin grafts, nearly 75% progress to form ectopic limbs (Table 2). A skin graft obtained from a site adjacent to the wound (ipsilateral) did not induce formation of ectopic limbs (Table 1).

Bump formation diverges from wound healing within the first few days

We used histological techniques to compare the early phases of bump formation induced by nerve deviation with regular wound healing. After the skin is removed, the epidermis surrounding the wound migrates to cover the wound surface within 2–4 h (trypan blue exclusion, see above). By 1 day after skin removal, the wound bed is covered by a well-formed epidermis that is one to two cell layers thick (Figs. 2A and E). By 5 days after wounding, the epidermis overlying the wound site is several cell layers thick and is distinct from the adjacent regions of normal skin (Figs. 2B and F). This localized region of thickened epidermis is induced in both the presence and absence of a deviated nerve, and appears comparable to the apical epidermal cap (AEC) that forms at the distal tip of an amputated limb (Wallace, 1981).

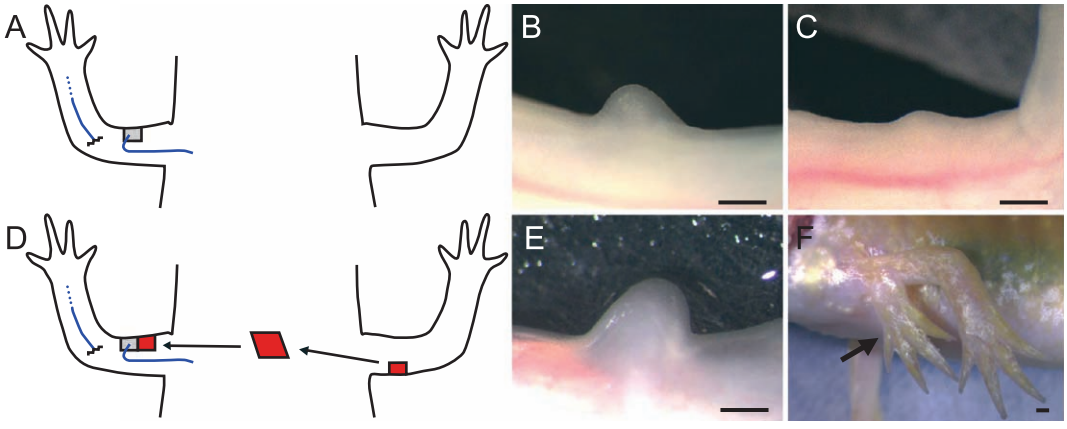

Fig. 1. Induction of bumps and ectopic limbs in response to wounding and nerve deviation. (A) A nerve is deviated into the superficial skin wound on the upper arm. The operation results in the formation of a bump (B; 13 days). Bumps eventually regress (C; 20 days). (D) A piece of skin from the opposite side of the contralateral limb is transplanted beside the skin wound to which a nerve is deviated. Bumps form at the wound site (E; 14 days) and continue to grow to form an ectopic limb (F; 5 months). Scale bars are 500 μm.

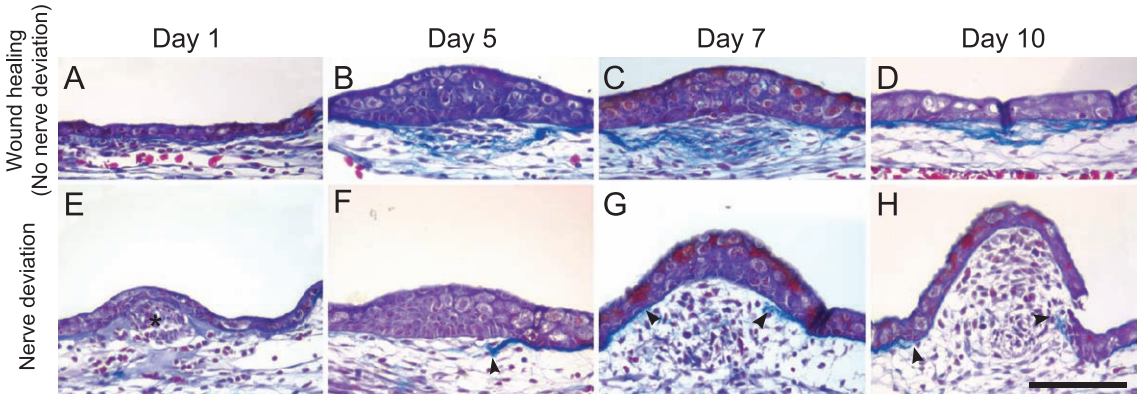

Fig. 2. Divergence of bump formation from the wound healing process. Sections of skin wounds (without nerve deviation; A–D) and bump formation (with nerve deviation; E–H) were stained with Mallory's triple stain at several time points after wounding; day 1 (A and E), day 5 (B and F), day 7 (C and G), and day 10 (D and H). Collagen fibers appear blue. The asterisk in E is a deviated nerve. Arrowheads (F, G, and H) indicate the edge of the dense collagen layer of the mature skin that was cut when the wound was made. Scale bar is 200 μm.

The first indication of a divergent response to the presence of a deviated nerve is evident at 5 days post-wounding. In the course of normal wound healing, a dense collagenous matrix, as evidenced by staining with aniline blue, is readily evident in the mesenchyme underlying the thickened epidermis (Fig. 2B). In contrast, in the presence of a deviated nerve, little or no matrix is seen within the connective tissue underlying the wound epidermis (Fig. 2F). This distinction between the two types of wounds becomes increasingly evident over the next several days. By day 7 of normal wound healing, the amount of collagenous matrix has increased in both volume and density (Fig. 2C). By day 10 of normal wound healing, the matrix appears to have been remodeled so as to restore the dense compact layer of collagenous fibers that underlie the epidermis of the mature skin (Fig. 2D). Over this same period of time, dense collagenous fibers are not observed underneath the wound epidermis in nerve-deviated wounds (arrowheads in Figs. 2F–H mark the unhealed edges of the dense collagenous layer). Overt evidence of bump formation—accumulated cells beneath the wound epidermis—can be observed histologically by 7 days in wounds with nerve grafts, but not in wounds alone (cf. Figs. 2C and G).

Proliferation induced by wounding increases as bumps grow

Based on BrdU incorporation, the proliferation rate of cells in uninjured limb dermal tissue is low (mean labeling index of 2.0%, SD = 1.7%, gray bar in Fig. 3 indicates the mean ± SD). In response to wounding, either in the presence or absence of a deviated nerve, the labeling index of dermal cells begins to increase, which we interpret to indicate that the proliferation rate of these cells is stimulated. In a normal wound without a deviated nerve, the labeling index of cells underlying the thickened epidermis (Fig. 2B) 5 days after wounding is about three times that of uninjured tissues (7.0%, Fig. 3E).

Although proliferation is stimulated by wounding without a deviated nerve, the presence of a nerve increases the rate of proliferation, even though a bump has yet to be formed. By day 5, the labeling index of cells beneath the thickened epidermis of nerve-deviated, pre-bump wounds (Fig. 2F) is already more than twice that of normal wounds, and nearly 10 times that of uninjured skin (Fig. 3A).

As bumps continue to grow, the rate of proliferation continues to increase and becomes spatially non-uniform within the bump. By day 7, a typical bump (Fig. 2G) is about 200 μm tall, and the labeling index has increased slightly compared to a pre-bump at day 5 (Fig. 3B). By day

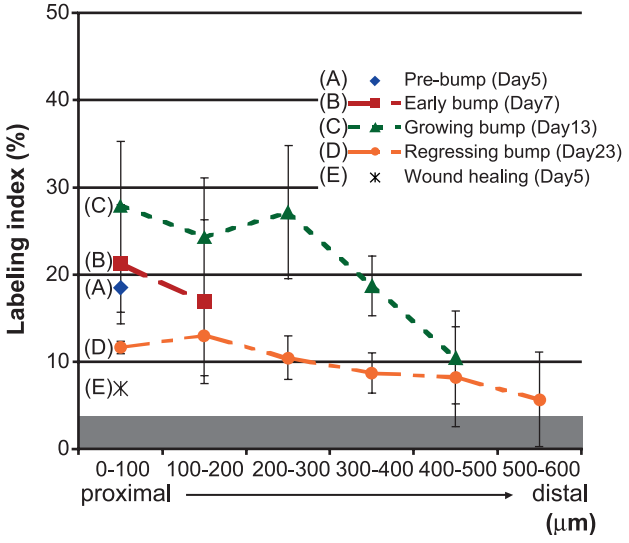

Fig. 3. Rates of cell proliferation during bump formation and regression. BrdU labeling indices are indicated for each 100-μm region of bumps with the most proximal region on the left of the graph and the most distal region on the right. Because bumps have not formed yet at pre-bump stage, we counted cells in the 100-μm region underneath the thickened epidermis. The labeling index is plotted in the 0- to 100-μm region for comparison. The gray area at the bottom of the graph represents the basal labeling index of uninjured skin (mean ± SD). Error bars indicate one standard deviation.

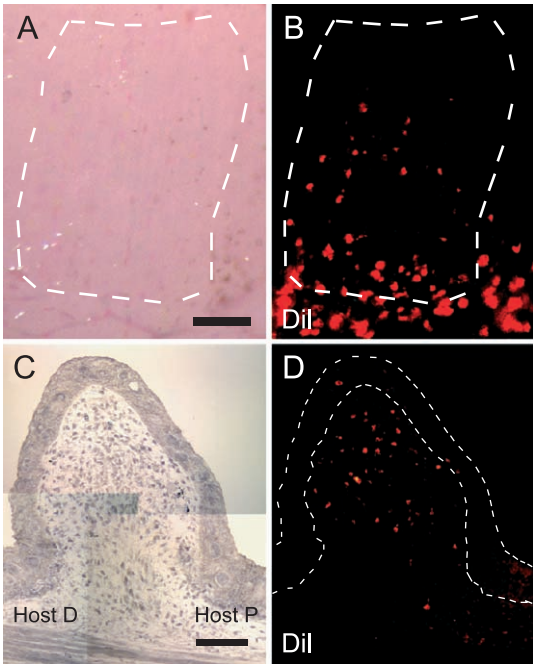

Fig. 4. Dermal fibroblast migration during wound healing and bump formation as viewed with DiI fluorescence. (A and B) Surface whole-mount view of a skin wound 3 days after wounding. (A) Bright field. (B) Fluorescence optics. Dashed lines indicate the boundary of the wound. DiI was injected into the mature dermal tissue at the bottom edge of the square. (C and D) Histological section of a day 21 bump. (C) Bright field. (D) Fluorescence optics. Dashed lines indicate the apical and basal layers of the epidermis. The orientation of the host limb is indicated as Host P (proximal) and Host D (distal). DiI was injected into the dermis at the proximal edge of the wound created on the host limb. Scale bars are 200 μm.

13, typical bumps are much larger (about 500 μm from base to distal tip) and show the highest rates of proliferation (LI of nearly 30%, Fig. 3C). Proliferation is uniformly high proximally and decreases significantly at the distal tip. The decrease in proliferation rate occurs in a graded fashion within the distal-most 200 μm such that the rate at the distal tip is only about a third that of the proximal rate and only slightly greater than that of uninjured tissues. This proximal to distal gradient of cellular proliferation is already evident in early bumps at day 7 (Fig. 3B).

Elevated levels of proliferation are not limited to the bump proper. Labeling indices on the order of 7% (mean LI = 6.8, SD = 3.5) are observed in connective tissue cells within a 400 μm periphery of the base of the bump (data not shown). Beyond this area, the LI of cells in the dermis is typical of uninjured tissues, indicating that 400 μm is the approximate limit of the range of mitogenic signals from the nerve and bump.

Growth of bumps is nerve-dependent as is the growth of regeneration blastemas. Bumps were denervated at 6 days (early stage) or 10 days (late stage) after nerve deviation. Bumps that were denervated at an early stage stopped growing within 2 days after denervation and were nearly completely regressed within another 2 days (four out of five; Figs. 5F–H). In contrast, bumps that were denervated at a late stage continued to grow for at least another 3 days (Figs. 5I and J). Denervated late stage bumps did begin to regress by 6 days after denervation (three out of four) and some had disappeared by 10 days (Figs. 5K and L).

Fibroblasts of the dermis contribute to bumps

By prelabeling dermal cells with DiI we determined that dermal fibroblasts surrounding the wound contribute to bumps. The migration of cells from the dermis adjacent to the wound begins before day 3 post-wounding (Figs. 4A and B). By 3 days, cells have already migrated to the center of a 1-mm square wound (Fig. 4B). Migration of cells from the peripheral dermis occurs whether or not a nerve has been deviated to the wound site.

By 21 days, a typical bump has formed, and many DiI-labeled cells can be observed in the mesenchyme of the bump (Figs. 4C and D). In the proximal region of the bump,

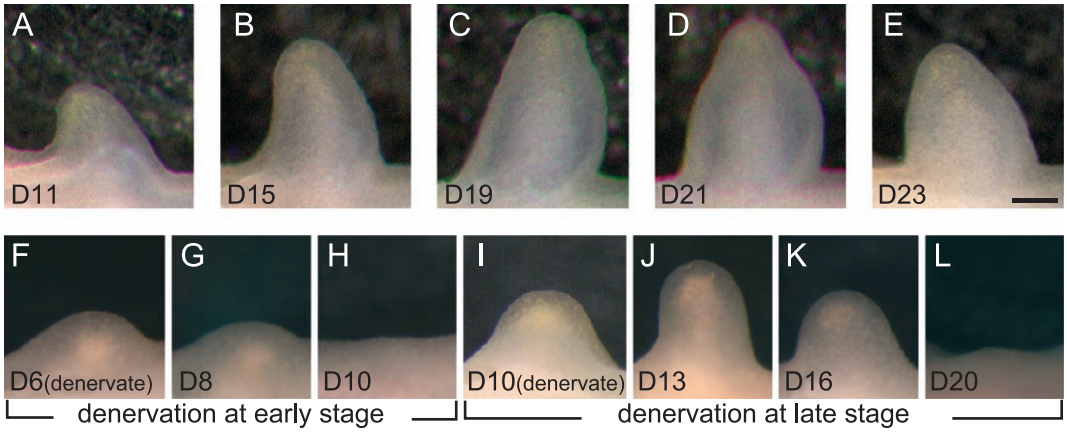

Fig. 5. Progressive stages of bump formation and regression (A–E). The bump grows (A and B), reaches its maximum size (C), expands laterally (D), and begins to regress (E). Bump regression after denervation of the host limb (F–L). Host limbs were denervated at day 6 (F–H) or day 10 (I–L) after wounding and nerve deviation to induce bump formation. A single bump was photographed at several times after induction (days) as indicated for each figure. Scale bar is 200 μm.

labeled mesenchymal cells are localized to the half of the bump adjacent to the position of the original labeled dermal fibroblasts. In contrast, in the distal bump labeled mesenchymal cells were uniformly distributed.

Bumps without skin grafts eventually regress

Although bumps induced by a deviated nerve go through a period of rapid growth, unless they also receive a contralateral skin graft (see below) they all eventually stop growing and undergo regression (Figs. 5A–E), leaving little or no evidence of the original bump (see Fig. 1C). This progression is similar for all the bumps we observed and is illustrated for a typical bump in Fig. 5. The bump grows to its maximal length by day 19 (Figs. 5A–C). By day 21, the bump had increased in volume by expanding laterally, without any increase in length (Fig. 5D). This lateral expansion is the first indication that a bump is beginning to regress, and it was observed in all bumps that subsequently regressed. Two days after expanding laterally (day 23), the bump had begun to decrease in height and thus was clearly regressing (Fig. 5E). On the basis of our observations, we determined that all bumps grow actively during the first 2 weeks after induction and are actively regressing 3 weeks after induction.

Coincident with the onset of regression, the rate of proliferation in older bumps decreases dramatically (Fig. 3). By day 23, during regression, proliferation rates have decreased to levels significantly lower than that of growing bumps and pre-bumps. The proximal to distal gradient in proliferation observed in growing bumps is still present, but is less steep. Consequently, the labeling index at proximal levels is still higher than in uninjured tissues, but at the distal tip proliferation has decreased to preinjury levels (Fig. 3).

We compared sections of growing and regressing bumps, and find that all growing bumps consist of undifferentiated mesenchymal cells and lack differentiated structures apart from a well-organized bundle of nerve fibers and associated connective tissue (Figs. 6A and E). Regressing bumps, however, contain a centrally located well-differentiated cartilage (Fig. 6B). A discrete mass of cells of unknown phenotype encapsulate the cartilaginous nodule and appear to extend proximally toward the base of the bump (Fig. 6B). These cells are negative for MF20 immunostaining (despite positive staining in control regenerating limbs; data not shown), an antibody that recognizes myosin light chain in myoblasts and myotubes (Bader et al., 1982), indicating that these are not myogenic cells.

The difference between growing and regressing bumps does not appear to be a consequence of a loss of innervation in regressing bumps. Both types of bumps are well innervated as determined by anti-acetylated tubulin immunohistochemistry (Figs. 6E and F). Regressing bumps exhibit a difference in the pattern of innervation in that many of the fibers encircle the cartilage nodule (Fig. 6G) before projecting into the distal tip. Because there is no nodule in growing bumps, nerve fibers extend distally without being impeded (Fig. 6E). Nevertheless, nerves innervate the distal epidermis in both types of bumps (Fig. 6H), though there could be subtle differences in the distribution of these

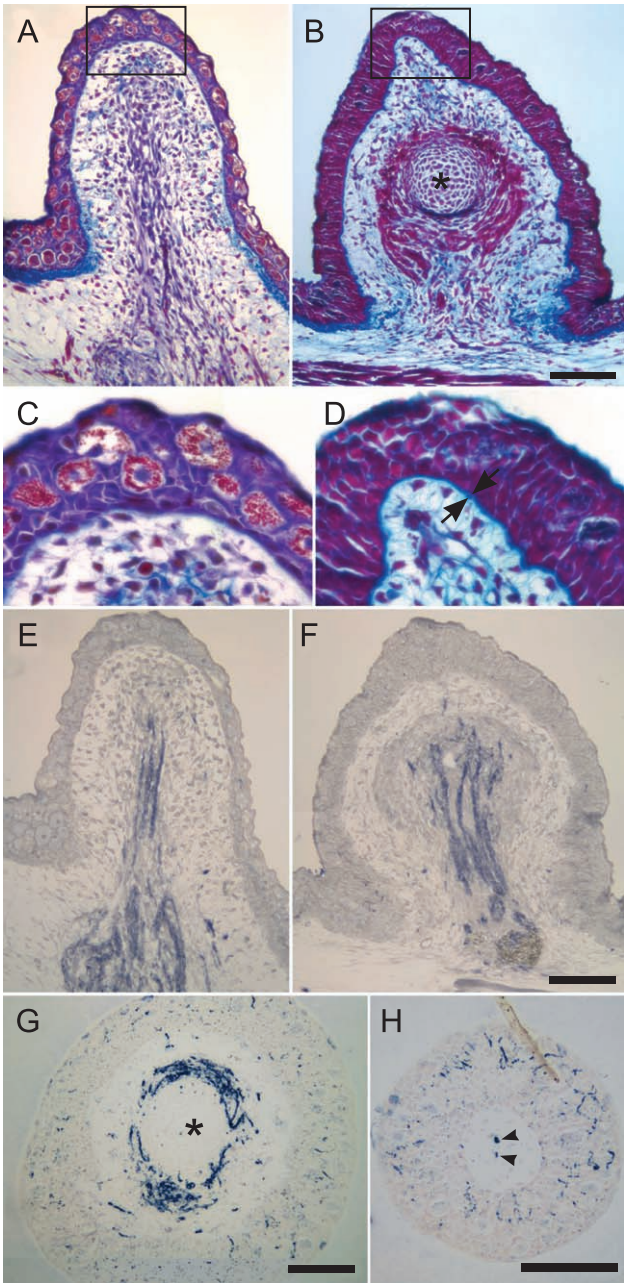

Fig. 6. Histological comparison of growing and regressing bumps. Adjacent sections have been stained by Mallory's triple stain (A–D) or anti-acetylated tubulin immunohistochemistry (E–H) for a growing bump (A and E) and a regressing bump (B and F). Images in C and D are a high magnification of squared areas in A and B, respectively. Images in G and H are transverse sections of a regressing bump at the distal tip (H) and at a level half-way between the base and the tip (G). Arrows (D) indicate the newly forming collagen layer underlying the apical epidermis of a regressing bump. Asterisks (B and G) indicate the sphere of cartilage present in regressing bumps. Arrowheads in H show nerves growing toward the distal tip. Scale bars are 200 μm.

smaller nerves that could influence the interaction between epidermal and mesenchymal cells.

A difference that might be relevant for regression is the degree to which the extracellular matrix (ECM) is redeveloped in regressing bumps. At proximal levels, the well-developed collagen layer of the mature skin is present in both types of bumps (Figs. 6A and B). At more distal levels, a discrete and continuous layer of collagen has redeveloped in regressing bumps (Fig. 6D). In contrast, no such layer of ECM is observable in growing bumps (Fig. 6C). The presence of this collagenous layer would presumably interfere with epithelial–mesenchymal interactions that are known to control outgrowth in regenerating limbs (Neufeld and Day, 1996).

Ectopic limb formation diverges from bump formation before the onset of regression

Rather than regressing, bumps that consist of cells from both anterior and posterior skin (anterior bumps with posterior skin grafts, and vice versa) go on to form a limb (Figs. 1F and 7; Table 2). Dermal fibroblasts from both host and graft skin contribute to nerve-induced bumps, which do not regress, but rather continue to develop into well-formed ectopic limbs at a high frequency.

In contrast to nerve-induced bumps, which regress 95% of the time, skin-grafted bumps formed limbs 73% of the time (Table 2). The frequencies of limb formation were comparable between anterior wounds with a posterior skin graft (7/9, 78%) and posterior wounds with an anterior skin graft (4/6, 67%). However, ectopic limbs induced at the site of an anterior wound were more complex structurally in comparison to limbs induced at the posterior site (Table 3). More than 70% of the anterior limbs formed at least four digits, the normal number of digits for an axolotl forelimb; whereas only 25% of the posterior limbs formed four digits.

Table 3
Complexity of ectopic limbs formed

Host site	Number of limbs	Two digits	Three digits	Four digits or >4[a]
Anterior	7	2	0	5
Posterior	4	2	1	1
Total	11	4	1	6

[a] Three animals formed duplicate ectopic limbs, which consist of more than four digits (the normal number of forelimb digits is four).

Skin-grafted bumps appear to progress through the same early stages of development as do bumps without a skin graft. During the growth stage of bumps (first 2 weeks, see above), the two types of bumps are indistinguishable externally (compare Figs. 1B and E). At the next stage of development, when a bump without a skin graft would expand laterally and begin to regress, a skin-grafted bump begins to flatten along the future dorsal–ventral axis (Fig. 7A) and become asymmetric along the future anterior–posterior axis (Fig. 7B). Over the next several weeks, skin-grafted bumps progress through developmental stages that are morphologically comparable to equivalent stages of both developing and regenerating axolotl limbs, and eventually form ectopic limbs with clearly identifiable skeletal elements (Figs. 7C and D).

Bumps that progress to form limbs differ histologically from regressing bumps. In contrast to symmetrical cartilaginous nodules formed in regressing bumps, anatomically

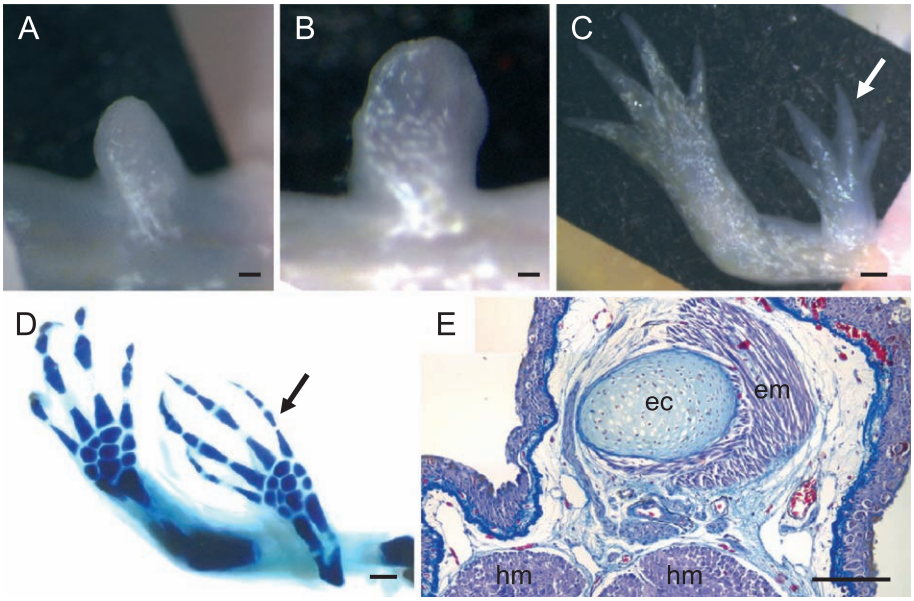

Fig. 7. Induction of an ectopic limb by nerve deviation and a skin graft. Three later stages of ectopic limb formation are illustrated on (A) day 17, (B) day 28, and (C) day 54 after induction. (D) Victoria Blue-stained skeletal preparation of an ectopic limb 5 months after induction. (E) A histological section of an ectopic limb (transverse section of the normal limb at the bottom). Tissues are indicated: ec, ectopic cartilage; em, ectopic muscle; hm, host muscle. Scale bars are 200 μm (A, B, and E) and 500 μm (C and D).

complex cartilaginous elements form that are comparable to those of normal axolotl limbs (Fig. 7E). As observed in previous studies (Maden and Holder, 1984), ectopic limbs are incomplete along the proximal–distal axis. A humerus is never formed, even though ectopic limbs were induced in the middle of the upper arm. Consequently, ectopic limbs are not connected to the host skeletal elements (Fig. 7D). Also, in contrast to regressing bumps, well-differentiated muscle fibers develop in ectopic limbs (three out of three limbs that were sectioned). As with the skeletal elements, the ectopic muscles are not connected to either the skeletal elements or muscles present in the host limb (Fig. 7E).

Discussion

Our results show that limb regeneration can be reproducibly induced by a series of experimentally supplied signals in an ectopic location, providing a stepwise experimental system for the analysis of regeneration (Fig. 8). The first of the signals is provided by nerves and is sufficient to turn a wound that would have regenerated only skin, into a bump, the equivalent of a regeneration blastema. The second signal(s) needed to turn a bump into a regenerate is provided by the interactions between fibroblasts with different positional identities. Being able to parse the regeneration process in this way, in an ectopic location, for the first time provides us with a positive assay for factors that are essential for regeneration. With this assay, we have the opportunity to identify the molecular signals that can change a wound into a blastema, and those that can turn a blastema away from a pathway of regression and onto a pathway of regeneration.

Bumps and blastemas

We have demonstrated that nerves provide the first essential step to ectopic regeneration by promoting the accumulation of regeneration-competent cells beneath the thickened wound epidermis (WE) at wound sites where otherwise there would have been no outgrowth. Regeneration following amputation is also dependent on nerves, and denervation before amputation or in the early blastema phase induces blastema regression and prevents regeneration (see Singer, 1952). Similarly, early stage bumps are dependent on nerves, and when denervated, they begin to regress immediately. With subsequent development, both late stage bumps and blastemas become less dependent, and eventually independent of nerves. Denervated late stage bumps continue to grow after denervation, and eventually regress, which is the fate of non-denervated bumps. Denervated late stage blastemas similarly do not regress, but their growth is inhibited and they eventually form a miniature regenerate. The nerve requirement is quantitative, and below a threshold number of nerves, neither bumps nor blastemas are formed (Bodemer, 1960; Singer, 1947). In both, nerves grow distally and innervate the apical epidermis, and in both bumps and regenerates, nerves appear to be involved directly or indirectly in regulating the growth permissive function of the epidermis. Several candidate molecules have been identified for the neurotrophic function of nerves in blastema forma-

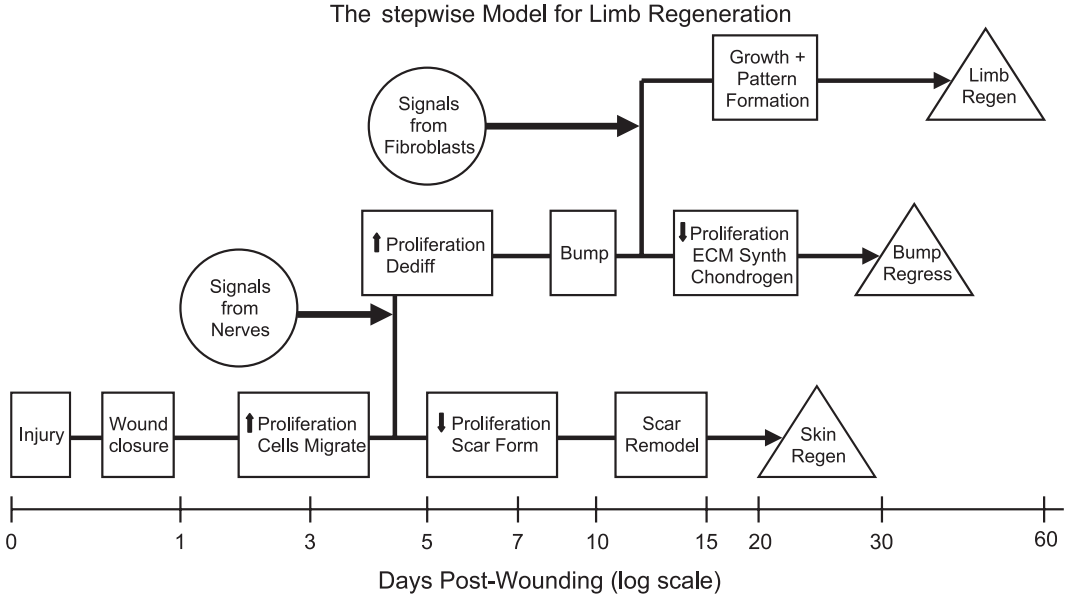

Fig. 8. The stepwise model for limb regeneration. The times after wounding (days) are represented on a logarithmic scale beginning on the left. The points of divergence of the three developmental pathways (wound healing, bump formation, and limb formation) are represented by vertical lines. The stepwise experimental system allows for the parsing of the overtly complex developmental process of limb regeneration so that each part (wound healing, dedifferentiation, and pattern formation) can be studied independently of the others. Abbreviations indicate: Regen, regeneration; Dediff, dedifferentiation; Synth, synthesis; Form, formation.

tion, including transferrin (Mescher and Munaim, 1984; Munaim and Mescher, 1986), glial growth factor (GGF) (Brockes and Kintner, 1986; Wang et al., 2000), and fibroblast growth factor 2 (FGF2) (Mescher and Gospodarowicz, 1979; Mullen et al., 1996). We previously demonstrated that nerves are a source of FGF in the early regenerating limb and that FGF2 can rescue regeneration in denervated limbs (Mullen et al., 1996).

Bumps and early blastemas are both derived from migrating dermal fibroblasts. In our studies, using DiI labeling, we show that dermal cells from the periphery of the wound migrate towards the wound center, starting at 3 days after wounding. When bumps have formed, DiI-labeled mesenchymal cells are localized proximally within the half of the bump that forms adjacent to the source of labeled fibroblasts. In contrast progeny of these fibroblasts is uniformly distributed in the distal region of the bump. This pattern of distribution of labeled cells suggests that cells surrounding the wound margin migrate uniformly toward, but not significantly beyond, the center of the wound. With subsequent growth and contribution to more distal regions of the outgrowth, cells become more homogeneously distributed. A similar mixing of dermal fibroblasts from opposite sides of the limb occurs during blastema formation, such that 75% of the cells remain on the side of origin and 25% become dispersed to the opposite side of the blastema (Muneoka et al., 1985; Rollman-Dinsmore and Bryant, 1984; Tank et al., 1985).

The range over which signals originating at wounding or amputation have their effect also appears to be similar for bumps and regenerates. We estimate the range of signals originating from amputation wounds to be not less than 100–150 μm. This is the distance from the amputation plane to the boundary in the stump of the early expression domains of *Hoxa-9* and *Hoxa-13* in connective tissues (Gardiner et al., 1995). For lateral wounds, we identified 400 μm as the range of signals from the wound that promote fibroblast entry into the cell cycle.

The cell cycle characteristics, as indicated by changes in labeling indices, of bumps and blastemas have several similarities. First, the onset of proliferation in both is coincident with the onset of cell migration (Gardiner et al., 1986; Maden, 1978). Second, as blastemas and bumps begin to elongate, a spatial heterogeneity in the pattern of cell proliferation is established, with the cells at the distal tip exhibiting a strikingly lower proliferation rate. During regeneration of both urodele limbs and fish fins, cells of the apical epidermis have a very long cell cycle, or may even be arrested in the cell cycle (Hay and Fischman, 1961; Poleo et al., 2001). Similarly, the distal-most blastema cells in regenerating urodele limbs have a long cell cycle compared to the cells at more proximal levels (Chalkley, 1954; Connelly and Bookstein, 1983), and a comparable population at the distal tip of regenerating fish fins has recently been observed (Nechiporuk and Keating, 2002). It is unclear whether cell cycle kinetics play a causal role in specification of the distal tip of the pattern, but it is likely that distal tip cells exhibit a unique pattern of gene expression because of their unique growth characteristics (Ohsugi et al., 1997). Experimental alterations in cell cycle kinetics can alter gene expression and pattern formation, and it has been hypothesized that a long cell cycle is characteristic of cells that function as signaling centers during embryonic development (Ohsugi et al., 1997).

Another important feature confirming that bumps are equivalent to early blastemas is that both have the ability to form complex patterns when provided with appropriate positional interactions, and fail to do so when they are not. This is also the case in regeneration of surgically created symmetrical limbs. Although all these amputated limbs form a blastema, most fail to form any structures, as in the situation with bumps without a skin graft (see Wallace, 1981). Hence, we infer that nerve-induced bumps that have not received a contralateral skin graft are equivalent to symmetrical limb blastemas. Thus, in a permissive environment controlled by both neurotrophic factors and outgrowth permitting signals from the WE (Muneoka et al., 1989), the amount of growth and pattern formation stimulated in both bumps and blastemas is quantitatively controlled by positional interactions between cells.

Finally, we presume that there are a multitude of similarities at the level of gene expression and protein function. This is almost certainly to be the case with regards to the control of cell migration and proliferation, and the response of fibroblasts to signals from nerves and the apical epidermis. It is also likely that formation of the proximal–distal axis of both bumps and blastemas will be governed by similar mechanisms because both form as outgrowths from a proximal source of cells derived from mature limb tissues. However, because bumps remain symmetrical in the absence of appropriate cell–cell interactions, we infer that there likely would be differences attributable to differences in anterior–posterior and dorsal–ventral patterning. However, when provided with skin grafts to stimulate such interactions in these axes, we presume that the same molecular mechanisms control formation of both ectopic limbs and regenerated limbs (Torok et al., 1998). The characterization of patterns of gene expression in bump formation is in progress.

Ectopic limbs exhibit a positional discontinuity between the proximal end of the ectopic limb and the proximal–distal level of the host limb from which they are induced. This phenomenon has been observed and discussed in detail previously (Maden and Holder, 1984). We note that ectopic limbs without a proximal–distal discontinuity can also be induced under some circumstances (Torok et al., 1998). In the original report on the induction of ectopic limbs (Bodemer, 1958), Bodemer reported (but did not clearly illustrate) that the ectopic limbs typically did form normal proximal structures, including the humerus. In the present study, as well as that of Maden and Holder (1984), we made every effort to avoid or minimize damage to the tissues of

the host limb when creating the wound and deviating the nerve. In contrast, Bodemer emphasized that he intentionally traumatized the tissues of the host limb. We therefore speculate that during the formation of ectopic limbs, dermal cells migrate and interact to form the distal part of the pattern first, which corresponds to the first phase of regeneration from an amputation (see Gardiner et al., 1986). However, in the absence of trauma, the host tissues are not induced to intercalate the most proximal parts of the pattern.

We conclude that bumps are equivalent to early blastemas that become arrested in development and regress in the absence of positional heterogeneity. Hence, bumps provide us with a novel and convenient stepwise model with which to discover the necessary and sufficient signals and conditions to control the migration and accumulation of fibroblasts into the blastema where they become the stem cells for the new limb, as well as the interactions between these cells that are essential for regeneration.

Acknowledgments

We wish to thank Mathieu Rondet for helpful comments on the manuscript and all the members of Bryant-Gardiner lab for helping and encouraging the research. The MF20 antibody was obtained from the Developmental Studies Hybridoma Bank, the University of Iowa. Research was supported by PHS grant HD-33465 (to S.V.B. and D.M.G) and the National Science Foundation through its support of the Axolotl Colony at Indiana University, Bloomington, IN.

References

Bader, D., Masaki, T., Fischman, D.A., 1982. Immunochemical analysis of myosin heavy chain during avian myogenesis in vivo and in vitro. J. Cell Biol. 95, 763–770.

Bodemer, C.W., 1958. The development of nerve-induced supernumberary limbs in the adult newt, *Triturus viridescens*. J. Morphol. 102, 555–581.

Bodemer, C.W., 1959. Observations on the mechanism of induction of supernumerary limbs in adult *Triturus viridescens*. J. Exp. Zool. 140, 79–99.

Bodemer, C.W., 1960. The importance of quantity of nerve fibers in development of nerve-induced supernumerary limbs in *Triturus* and enhancement of the nervous influence by tissue implants. J. Morphol. 107, 47–59.

Brockes, J.P., Kintner, C.R., 1986. Glial growth factor and nerve-dependent proliferation in the regeneration blastema of urodele amphibians. Cell 45, 301–306.

Bryant, S.V., Endo, T., Gardiner, D.M., 2002. Vertebrate limb regeneration and the origin of limb stem cells. Int. J. Dev. Biol. 46, 887–896.

Carlson, M.R.J., Bryant, S.V., Gardiner, D.M., 1998. Expression of *Msx-2* during development, regeneration, and wound healing in axolotl limbs. J. Exp. Zool. 282, 715–723.

Chalkley, D.T., 1954. A quantitative histological analysis of forelimb regeneration in *Triturus viridescens*. J. Morphol. 94, 21–70.

Connelly, T.G., Bookstein, F.L., 1983. Method for 3-dimensional analysis of patterns of thymidine labeling in regenerating and developing limbs. Prog. Clin. Biol. Res. 110 Pt. A, 525–536.

Egar, M.W., 1988. Accessory limb production by nerve-induced cell proliferation. Anat. Rec. 221, 550–564.

Gardiner, D.M., Muneoka, K., Bryant, S.V., 1986. The migration of dermal cells during blastema formation in axolotls. Dev. Biol. 118, 488–493.

Gardiner, D.M., Blumberg, B., Komine, Y., Bryant, S.V., 1995. Regulation of HoxA expression in developing and regenerating axolotl limbs. Development 121, 1731–1741.

Gardiner, D.M., Carlson, M.R.J., Roy, S., 1999. Towards a functional analysis of limb regeneration. Semin. Cell Dev. Biol. 10, 385–393.

Gardiner, D.M., Endo, T., Bryant, S.V., 2002. The molecular basis of amphibian limb regeneration: integrating the old with the new. Semin. Cell Dev. Biol. 13, 345–352.

Hay, E.D., Fischman, D.A., 1961. Origin of the blastema in regenerating limbs of the newt *Triturus viridescens*. An autoradiographic study using tritiated thymidine to follow cell proliferation and migration. Dev. Biol. 3, 26–59.

Humason, G.L., 1979. Animal Tissue Techniques. Freeman, San Francisco.

Lheureux, E., 1977. Importance of limb tissue associations in the development of nerve-induced supernumerary limbs in the newt *Pleurodeles waltlii* Michah. J. Embryol. Exp. Morphol. 1977, 151–173.

Li, S., Muneoka, K., 1999. Cell migration and chick limb development: chemotactic action of FGF-4 and the AER. Dev. Biol. 211, 335–347.

Maden, M., 1978. Neurotrophic control of the cell cycle during amphibian limb regeneration. J. Embryol. Exp. Morphol. 48, 169–175.

Maden, M., Holder, N., 1984. Axial characteristics of nerve induced supernumerary limbs in the axolotl. Roux's Arch. Dev. Biol. 193, 394–401.

Mescher, A.L., Gospodarowicz, D., 1979. Mitogenic effects of a growth factor derived from myelin on denervated regenerates of newt forelimbs. J. Exp. Zool. 207, 497–503.

Mescher, A.L., Munaim, S.I., 1984. Trophic effect of transferrin on amphibian limb regeneration blastemas. J. Exp. Zool. 230, 485–490.

Mullen, L., Bryant, S.V., Torok, M.A., Blumberg, B., Gardiner, D.M., 1996. Nerve dependency of regeneration: the role of Distal-less and FGF signaling in amphibian limb regeneration. Development 122, 3487–3497.

Munaim, S.I., Mescher, A.L., 1986. Transferrin and the trophic effect of neural tissue on amphibian limb regeneration blastemas. Dev. Biol. 116, 138–142.

Muneoka, K., Holler-Dinsmore, G.V., Bryant, S.V., 1985. A quantitative analysis of regeneration from chimaeric limb stumps in the axolotl. J. Embryol. Exp. Morphol. 90, 1–12.

Muneoka, K., Bryant, S.V., Gardiner, D.M., 1989. Growth control in limb regeneration. In: Armstrong, J.B., Malacinsky, G.M. (Eds.), Developmental Biology of the Axolotl. Oxford Univ. Press, New York, pp. 143–156.

Nechiporuk, A., Keating, M.T., 2002. A proliferation gradient between proximal and *msxb*-expressing distal blastema directs zebrafish fin regeneration. Development 129, 2607–2617.

Neufeld, D.A., Day, F.A., 1996. Perspective: a suggested role for basement membrane structures during newt limb regeneration. Anat. Rec. 246, 155–161.

Ohsugi, K., Gardiner, D.M., Bryant, S.V., 1997. Cell cycle length affects gene expression and pattern formation in limbs. Dev. Biol. 189, 13–21.

Poleo, G., Brown, C.W., Laforest, L., Akimenko, M.A., 2001. Cell proliferation and movement during early fin regeneration in zebrafish. Dev. Dyn. 221, 380–390.

Reynolds, S., Holder, N., Fernandes, M., 1983. The form and structure of supernumberary hindlimbs formed following skin grafting and nerve deviation in the newt *Triturus cristatus*. J. Embryol. Exp. Morphol. 77, 221–241.

Rollman-Dinsmore, C., Bryant, S.V., 1984. The distribution in limb regenerates of marked dermal cells from small localized implants. Dev. Biol. 106, 275–281.

Singer, M., 1947. The nervous system and regeneration of the forelimb of

adult *Triturus*: VI. A further study of the importance of nerve number, including quantitative measurements of limb innervation. J. Exp. Zool. 104, 223–249.

Singer, M., 1952. The influence of the nerve in regeneration of the amphibian extremity. Quart. Rev. Biol. 27, 169–200.

Tank, P.W., Connelly, T.G., Bookstein, F.L., 1985. Cellular behavior in the anteroposterior axis of the regenerating forelimb of the axolotl, *Ambystoma mexicanum*. Dev. Biol. 109, 215–223.

Torok, M.A., Gardiner, D.M., Shubin, N.H., Bryant, S.V., 1998. Expression of *HoxD* genes in developing and regenerating axolotl limbs. Dev. Biol. 200, 225–233.

Wallace, H., 1981. Vertebrate Limb Regeneration. Wiley, Chichester.

Wang, L., Marchionni, M.A., Tassava, R.A., 2000. Cloning and neuronal expression of a type III newt neuregulin and rescue of denervated, nerve-dependent newt limb blastemas by rhGGF2. J. Neurobiol. 43, 150–158.